Journal of Materials Chemistry A

PAPER

View Article Online
View Journal | View Issue

Cite this: J. Mater. Chem. A, 2015, 3, 15292

Functionalized metal–organic framework as a new platform for efficient and selective removal of cadmium(II) from aqueous solution†

Yang Wang,*[ab] Guiqin Ye,[a] Huanhuan Chen,[a] Xiaoya Hu,[a] Zheng Niu[b] and Shengqian Ma*[b]

Received 1st May 2015
Accepted 26th June 2015

DOI: 10.1039/c5ta03201f

www.rsc.org/MaterialsA

In this work, we illustrate how to anchor $-SO_3H$ functional groups onto the pore surface of MOF for cadmium removal from aqueous solution *via* the approach of sequential post-synthetic modification and oxidation as exemplified in the context of functionalizing the MOF, $Cu_3(BTC)_2$ with sulfonic acid. The resultant sulfonic acid functionalized MOF, $Cu_3(BTC)_2-SO_3H$ demonstrates a high cadmium uptake capacity of 88.7 mg g^{-1}, surpassing that of the benchmark adsorbents. In addition, it exhibits a fast kinetics with the kinetic rate constant k_2 of 0.6818 g mg^{-1} min, which is 1–3 orders of magnitude higher than existing adsorbent materials for adsorbing cadmium ions from aqueous solution. Moreover, it demonstrates high selectivity of cadmium ions in the presents of other background metal ions, and can be readily regenerated and recycled without significant loss of cadmium uptake capacity. Our work thus paves a way for developing functionalized MOFs as a new type of platform for removing cadmium from wastewater.

1. Introduction

Heavy metal pollution particularly in aqua systems, due to the rapid increase of industrial and mining activities, has become a serious threat to environment and public health.[1] Heavy metal ions, even at low concentrations, are highly toxic to living organisms. Heavy metal ions are non-biodegradable, and they tend to accumulate in the environment thus exerting the negative affect on the environments and ecosystems.[2,3] In particular, cadmium is known to directly damage the nervous, reproductive, renal, and skeletal systems, and can also cause some cancers.[4,5] Therefore, the efficient removal of cadmium from wastewater disposed from industrial and mining processes is of urgent need.

A variety of methods for cadmium removal from wastewater have been explored over the past.[6,7] Among those methods, adsorption stands out considering its comparatively low cost, simple design, easy operation, and facile regeneration.[8,9] Various types of sorbent materials, such as carbon materials,[10,11] biomass,[12] magnetic nanoparticles,[13] and chelating polymers[14] have been extensively investigated for adsorptive removal of cadmium from contaminated water. However, those sorbents face sorts of challenges such as the low surface area, low capacity, moderate affinity/selectivity for Cd(II), which have largely limited their effectiveness and efficiency for the removal of Cd(II) from aqueous solutions. The weaknesses and handicaps associated with existing adsorbents necessitate the development of new types of materials for highly effective and highly efficient removal of Cd(II) from aqueous solutions.

Over the past decade, metal–organic frameworks (MOFs) have emerged as a new type of porous materials and have demonstrated great potential for applications in gas adsorption, gas separation, catalysis, and lithium storage.[15–19] The employment of MOFs for remove heavy metal ions from aqueous solutions has recently exploited with focus on introducing thio/thiol-functional groups into MOFs for the removal of mercury and lead ions.[20–23] Nonetheless, the exploration of MOFs for cadmium(II) removal particularly selective removal of Cd(II) from other metal ions that remains a challenge to be addressed, has not yet been reported. In this contribution, we illustrate how to anchor the $-SO_3H$ functional groups onto the pore surface of MOF *via* the approach of sequential post-synthetic modification and oxidation, and the resultant sulfonic acid functionalized MOF demonstrates high uptake capability and fast kinetics for cadmium removal from aqueous solution as well as high selectivity of cadmium ions in the presents of other background metal ions.

2. Experimental section

2.1. Apparatus

A Zeenit 700 atomic absorption spectrometer (Germany) equipped with a flame atomizer was employed for the determination

[a]School of Chemistry and Chemical Engineering, Yangzhou University, Yangzhou 225002, China. E-mail: wangyzu@126.com

[b]Department of Chemistry, University of South Florida, 4202 East Fowler Avenue, Tampa, Florida 33620, USA. E-mail: sqma@usf.edu

† Electronic supplementary information (ESI) available: Zeta potential, adsorption isotherms, and adsorption kinetics parameters. See DOI: 10.1039/c5ta03201f

of cadmium concentration. A cadmium hollow cathode lamp was used as the radiation source at 282.1 nm. Measurements were carried out in the integrated absorbance (peak area) mode at 6 mA, using a spectral bandwidth of 0.2 nm. A Tensor 27 spectrometer (Bruker Co., Germany) was used to obtain Fourier transforms infrared (FTIR) spectra. Powder X-ray diffraction (PXRD) patterns were recorded on a D8 Advance X-ray Diffractometer (Germany) at room temperature. Field emission scanning electron micrographs (SEM) were obtained with a Hitachi S-4800 microscope (Japan) at an acceleration voltage of 15 kV. Specific surface area (BET) was measured by Quantachrome Company NOVA/4000 E physical adsorption instrument automation by N_2 sorption at 77 K.

2.2. Reagents and materials

The cadmium stock solution of 1000 mg L^{-1} was prepared by dissolving 0.1633 g of $CdCl_2 \cdot 2H_2O$ in 100 mL deionized water. Working standard solutions of cadmium were prepared by stepwise dilution of the stock solution with deionized water. Copper nitrate, 1,3,5-benzene tricarboxylic acid (H_3BTC, 98%), and other reagents were of analytical reagent grade and obtained from Sinopharm Chemical Reagent Co., Ltd. Double deionized water (18 MΩ cm) was used throughout the experiments.

2.3. Preparation of $Cu_3(BTC)_2$

The fabrication process was prepared from a typical synthesis method after minor modifications:[17] 0.2178 g (0.9 m mol) $Cu(NO_3)_2 \cdot 3H_2O$ was dissolved in 3 mL de-ionized water and mixed with 0.0945 g (0.5 m mol) of H_3BTC dissolved in 6 mL ethanol. The solution was added to a 20 mL Teflon liner, placed in an autoclave, and heated to 393 K for 12 h. The crystals obtained were then filtered, washed with water and ethanol, and dried in 60 °C.

2.4. Preparation of thiol functionalized $Cu_3(BTC)_2$

The thiol functionalized $Cu_3(BTC)_2$ were prepared according to the previous report:[20] 0.1 g as-synthesized $Cu_3(BTC)_2$ sample was dehydrated at 150 °C for 12 h, and suspended in 10 mL of anhydrous toluene. 1 mL 0.24 mol L^{-1} dithioglycol solution was then added, and the mixture solution was stirred magnetically for 24 h at room temperature. The solution was filtered, washed by ethanol, and dried in 60 °C. The reaction mechanism diagram was shown in Scheme 1 (ESI†).

2.5. Preparation of sulfonic functionalized $Cu_3(BTC)_2$

1 g thiol functionalized $Cu_3(BTC)_2$ sample was dissolved in 50 mL methanol, and sonicated for 10 minutes. 16.3 mL hydrogen peroxide (30%) was added and stirred for 8 hours. Furthermore, the solution was acidified with 0.1 mol L^{-1} H_2SO_4 for 4 h to ensure complete protonation of all sulfonic acid groups. The resulting crystals were washed by water and ethanol, and dried in 60 °C.

2.6. Adsorption and desorption studies

The adsorption of cadmium by the $Cu_3(BTC)_2$–SO_3H was investigated using batch equilibrium technique in aqueous solutions, and the pH of the solution was adjusted to 6 with 0.1 mol L^{-1} HNO_3 or 0.1 mol L^{-1} NaOH solutions. In general, 10 mg of $Cu_3(BTC)_2$–SO_3H adsorbent was added to 10 mL of sample solution containing cadmium and shaken at room temperature for 10 min to facilitate adsorption of cadmium onto the sorbent. Desorption was then studied by adding 0.5 mL 0.50 mol L^{-1} of nitric acid solution to the cadmium-sorbed $Cu_3(BTC)_2$–SO_3H. After shaking at 200 rpm for 10 min, the $Cu_3(BTC)_2$–SO_3H were removed and the concentration of cadmium was measured using atomic absorption spectrometer. In order to obtain the adsorption isotherms of the cadmium, solutions with varying initial concentration of cadmium were treated with the same procedure as above at room temperature. The removal efficiency and the amount of heavy metal ions adsorbed q (mg g^{-1}) were given according to the formula:

$$\text{Removal efficiency } (\%) = \frac{c_o - c_e}{c_o} \times 100\% \quad (1)$$

where c_o and c_e (mg L^{-1}) are the initial and equilibrium concentrations of cadmium in the solution, respectively.

3. Results and discussion

3.1. Characterization of the sorbent

Given its large surface area, high pore volume, reasonable water/chemical stability, and the accessibility of exposable copper sites for the surface functionalization, we selected $Cu_3(BTC)_2$ (BTC = 1,3,5-benzenetricarboxylate)[24,25] as a platform to anchor the sulfonic groups that are known to form a stable complex with cadmium ion[26] for cadmium removal from aqueous solutions. To introduce sulfonic groups onto the pore surface of $Cu_3(BTC)_2$, the dithioglycol was first grafted to the open copper sites of the paddle wheel secondary building blocks (SBUs) followed by oxidation of the dangled thiol groups with hydroperoxide (Fig. 1) (hereafter $Cu_3(BTC)_2$–SO_3H). The successful anchoring of sulfonic groups has been confirmed by FTIR studies, which reveal the appearance of the characteristic

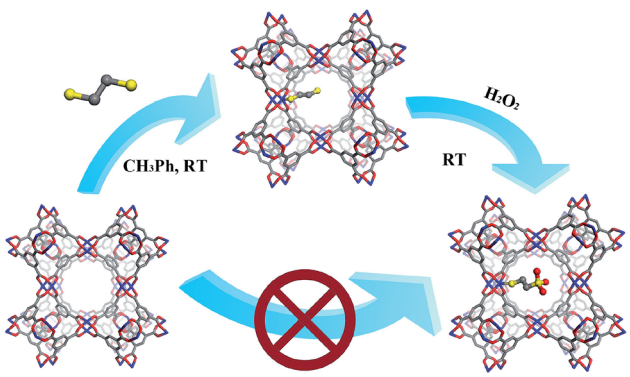

Fig. 1 Introduction of sulfonic groups into $Cu_3(BTC)_2$ *via* step-wise post-synthetic modification.

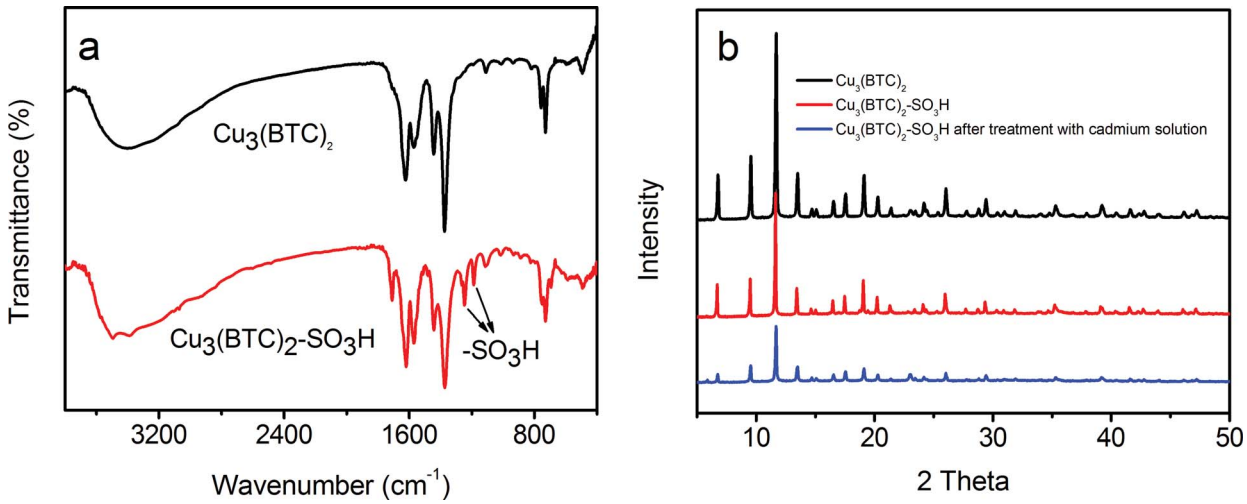

Fig. 2 FTIR spectra (a) and PXRD patterns (b) of $Cu_3(BTC)_2$ and $Cu_3(BTC)_2$–SO_3H.

Table 1 BET surface areas and pore volumes of $Cu_3(BTC)_2$ and $Cu_3(BTC)_2$–SO_3H

Specimens	Surface area ($m^2\ g^{-1}$)	Pore volume ($cm^3\ g^{-1}$)
$Cu_3(BTC)_2$	627	0.301
$Cu_3(BTC)_2$–SO_3H	445	0.300

stretching vibration peaks of S–O band[27,28] between 1000–1350 cm^{-1} $Cu_3(BTC)_2$–SO_3H compared with $Cu_3(BTC)_2$ (Fig. 2a). The preservation of structural integrity after the introduction of sulfonic groups has been verified by the consistence in the powder X-ray diffraction (PXRD) patterns of $Cu_3(BTC)_2$ and $Cu_3(BTC)_2$–SO_3H (Fig. 2b).[29] PXRD patterns before and after treatment with cadmium solution also indicate that the introduction of –SO_3H functional groups can improve the water-stability of $Cu_3(BTC)_2$. The SEM image (Fig. S1, ESI†) for $Cu_3(BTC)_2$ shows octahedral crystals with smooth surfaces. Although the shape and size of $Cu_3(BTC)_2$–SO_3H before and after treatment with cadmium solution are similar to $Cu_3(BTC)_2$, the structure of $Cu_3(BTC)_2$–SO_3H is more loose. The Brunauer–Emmett–Teller (BET) surface areas and pore volumes were derived from nitrogen adsorption isotherms at 77 K and the results are presented in Table 1. Compared with $Cu_3(BTC)_2$, the BET surface area of $Cu_3(BTC)_2$–SO_3H was reduced to 445 $m^2\ g^{-1}$, further indicating that successful grafting of –SO_3H groups on the pore surface of $Cu_3(BTC)_2$.

3.2. Investigation of the effects of pH value in solution on cadmium adsorption and proposed adsorption mechanism

The adsorption of heavy metal ions depends on the pH value of the solution because pH may change the speciation of metal ions and the surface charges of the adsorbent. The obtained zeta potential value of $Cu_3(BTC)_2$–SO_3H decreased with the increase in solution pH, and the isoelectrical point (IEP) was about 2.1 (Fig. S1, ESI†). Based on these data, the adsorption at pH < 2.1 would be unfavorable for metal cations due to the repulsion with the positively charged surface of the $Cu_3(BTC)_2$–SO_3H adsorbent. The effect of the initial solution pH on the adsorption of cadmium ions onto $Cu_3(BTC)_2$–SO_3H composites was then studied in the range of 3.0–8.0 as shown in Fig. 3. The removal efficiency capacity improves with increasing pH values from 3.0 to 6.0. Increasing pH values above 6.0 leads to gradual decrease in the adsorption capacity. At lower pH values (pH < 3.0), protons could occupy most of the adsorption sites on the adsorbent surface, and hence only a low amount of cadmium can be adsorbed due to the competition between protons and cadmium ions. Above pH 6.0, cadmium would precipitate to form hydroxide salts, thus to weaken the interactions between –SO_3H groups and cadmium ions. Therefore, an optimal pH of 6.0 was selected for all adsorption studies. Fig. 4 illustrates the proposed mechanism for the adsorption of cadmium ions in $Cu_3(BTC)_2$–SO_3H, which suggests that the metal ions interact with the adsorbent mainly by chelation between the metal ions and the –SO_3H groups.

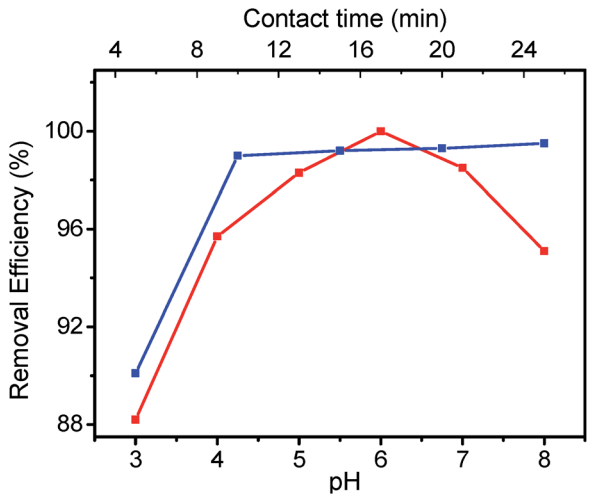

Fig. 3 Effect of solution pH (red line) and contact time (blue line) on cadmium(II) adsorption in $Cu_3(BTC)_2$–SO_3H.

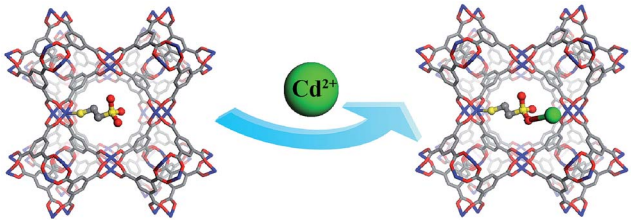

Fig. 4 Proposed mechanism for Cd(II) adsorption in $Cu_3(BTC)_2$–SO_3H.

The contact time also significantly influences the adsorption rate of the target ions. In order to achieve the saturation uptake capacity, the effects of contact time on the adsorption were investigated in the range of 5–25 min. As shown in Fig. 3, there is no significant change in the removal efficiency of cadmium after 10 min contact time. Compared with other reported adsorbents,[13,30–34] $Cu_3(BTC)_2$–SO_3H shows a fast adsorption rate for Cd(II) ions. Such high efficiency could be attributed to the large surface area of $Cu_3(BTC)_2$ and the high density of –SO_3H groups grafted on the $Cu_3(BTC)_2$. The contact time of 10 min was then selected for further investigations.

3.3. Cadmium adsorption isotherms

To estimate the cadmium(II) uptake capacity of $Cu_3(BTC)_2$–SO_3H, the adsorption isotherms of cadmium were collected from solutions containing different initial cadmium concentrations (0–200 mg L^{-1}) under the optimized experimental conditions of 10 min-contact time and pH 6.0. The experimental adsorption isotherm data were then fitted with Langmuir and the Freundlich equations to derive the adsorption capacity and affinity of $Cu_3(BTC)_2$–SO_3H for Cd(II) ions.

The Langmuir isotherm model can be described as the following equation:[35]

$$\frac{c_e}{q_e} = \frac{c_e}{q_m} + \frac{1}{q_m K_L} \quad (2)$$

where q_e is the amount of cadmium adsorbed on the adsorbent at equilibrium (mg g^{-1}), c_e is the equilibrium cadmium concentration in the solution (mg L^{-1}), q_m is the maximum adsorption capacity at monolayer coverage (mg g^{-1}), and K_L is the Langmuir constant, quantitatively reflecting the affinity of binding sites (L mg^{-1}) to energy of adsorption. The Langmuir model assumes that the solid surface active sites can be occupied only by one layer of adsorbates and that the active sites are independent.

On the contrary, the Freundlich model is based on a heterogeneous adsorption. The Freundlich isotherm is given as:[36]

$$\ln q_e = \ln K_F + \frac{1}{n} \ln c_e \quad (3)$$

where q_e (mg g^{-1}) and c_e (mg L^{-1}) have the same definitions as above mentioned. K_F is the Freundlich constant which indicates the adsorption capacity (L g^{-1}), and n is an empirical parameter related to the intensity of adsorption.

The relationship between initial cadmium concentration and the adsorption capacity was analyzed using both the Langmuir and Freundlich models (Fig. 5). The calculated correlation coefficient (q_m, K_L, K_F, and n) and linear regression coefficient (R^2) values for each model were shown in Table S1 (ESI†). With respect to the correlation coefficients (R^2) values, the Langmuir isotherm generates a more satisfactory fit to the experimental data than the Freundlich isotherm with the R^2 value greater than 0.998. This suggests that the adsorption of cadmium by $Cu_3(BTC)_2$–SO_3H is monolayer-type and agrees with the observation that the adsorption from an aqueous solution usually forms a layer on the adsorbent surface.

The maximum uptake capacity (q_m) for cadmium(II) ions derived from the Langmuir equation is 88.7 mg g^{-1}. To highlight the contribution of –SO_3H groups to cadmium uptake, we compared the adsorption isotherms of parent $Cu_3(BTC)_2$, $Cu_3(BTC)_2$–SH, and $Cu_3(BTC)_2$–SO_3H. $Cu_3(BTC)_2$–SO_3H outperforms both $Cu_3(BTC)_2$ and $Cu_3(BTC)_2$–SH, which exhibit a cadmium uptake capacity of 67.8 mg g^{-1} and 74.5 mg g^{-1} respectively despite its lower surface area. The lower cadmium adsorption capacity observed for $Cu_3(BTC)_2$ could be attributed to that cadmium ions are adsorbed from the solution phase onto the surface of the $Cu_3(BTC)_2$ by selective complexation with residual carboxyl groups. The introduction of –SH groups, favorable for cadmium binding, on the surface of $Cu_3(BTC)_2$,

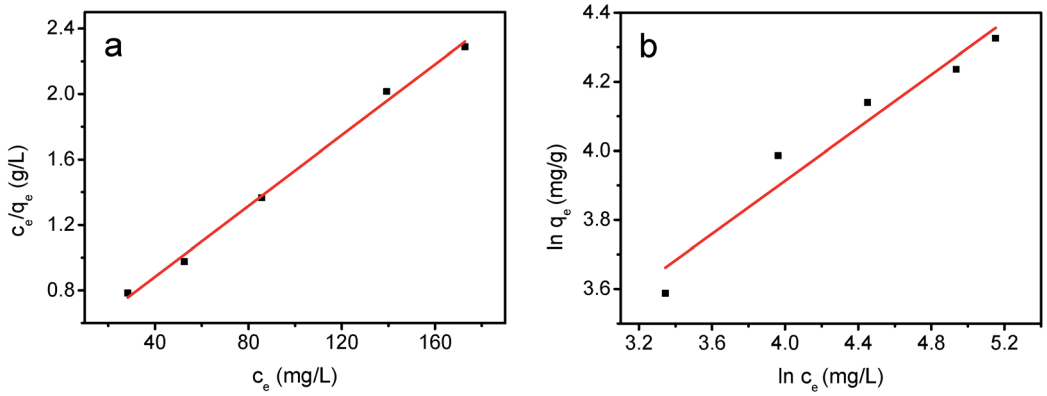

Fig. 5 Langmuir (a) and Freundlich (b) fitting for the adsorption of cadmium onto $Cu_3(BTC)_2$–SO_3H.

Table 2 Comparison of cadmium adsorption performances by various adsorbents[a]

Sorbent	Adsorption capacity (mg g^{-1})	Adsorption time (min)	Functionalized groups	Reuse times	Ref.
Fe_3O_4@APS@AA-*co*-CA	29.6	45	Carboxyl	4	13
Sulfonic-functionalized poly (dimethylsiloxane) networks	78.7	1440	Sulfonic acid	ND	30
Salicylic acid type chelate	45.0	120	Carboxyl, amine, and hydroxyl	10	31
Magnetic yeast treated with EDTA dianhydride	48.7	30	Carboxyl, and amine	3	32
PPBM	43.5	100	ND	ND	33
Si–DTC	40.5	60	Dithiocarbamate	ND	34
MPGI	87.7	1	Carboxyl	15	39
ZrO_2/B_2O_3	109.9	30	ND	100	40
$Cu_3(BTC)_2$–SO_3H	88.7	10	Sulfonic acid	6	This work

[a] Fe_3O_4@APS@AA-*co*-CA: Fe_3O_4 magnetic nanoparticles modified with 3-aminopropyltriethoxysilane and copolymers of acrylic acid and crotonic acid; PPBM: Portulaca plant biomass; Si-DTC: Silica-supported dithiocarbamate adsorbent; MPGI: magnetic Fe_3O_4–glycidyl methacrylate–iminodiacetic acid–styrene–divinyl benzene resin; ND: not reported.

leads to the improvement of cadmium adsorption capacity. Whereas, an further enhanced has been achieved after oxidizing the dangled thiol groups into sulfonic groups for $Cu_3(BTC)_2$–SO_3H presumably because –SO_3H groups can provide multiple binding sites and versatile coordination modes for Cd(II) ions.[37,38] It is worth noting that the cadmium uptake capacity of $Cu_3(BTC)_2$–SO_3H surpasses that of a series of benchmark sorbent materials (Table 2),[13,30–34,39,40] highlighting its potential for application in wastewater treatment.

3.4. Kinetics of cadmium adsorption

It's known that the adsorption process of heavy metal ions depends on an amalgam of multiple mechanisms such as mass transfer, diffusion control, chemical reactions and particle diffusion. In order to understand the cadmium adsorption kinetics in $Cu_3(BTC)_2$–SO_3H, the experimental data collected at the initial cadmium concentration of 1 mg L^{-1} in pH 6.0 were fitted with the Lagergren pseudo-first-order kinetic model and pseudo-second-order kinetic model.

The pseudo-first-order and pseudo-second-order kinetic models can be described as:[41,42]

$$\ln (q_e - q_t) = \ln (q_e) - k_1 t \quad (4)$$

$$\frac{t}{q_t} = \frac{1}{k_2 q_e^2} + \frac{t}{q_e} \quad (5)$$

where q_e (mg g^{-1}) and q_t (mg g^{-1}) are the amounts of the metal ions adsorbed at equilibrium and at time t (min), respectively; k_1 (min^{-1}) and k_2 ((g mg^{-1}) min^{-1}) are the kinetic rate constants for the pseudo-first-order and the second-order models, respectively. The validities of these two kinetic models are examined and depicted in Fig. 6, and the values of the parameters and the correlation coefficients obtained from these two kinetic models are all listed in Table S2 (ESI†). The results suggest that the cadmium adsorption process in $Cu_3(BTC)_2$–SO_3H follow the pseudo-second-order kinetic model instead of the pseudo-first-order model. The derived kinetic rate constant k_2 was calculated to be 0.6818 g mg^{-1} min, which is 1–3 orders of magnitude higher than other adsorbent materials in the cadmium adsorption under similar conditions.[32–34,43–47]

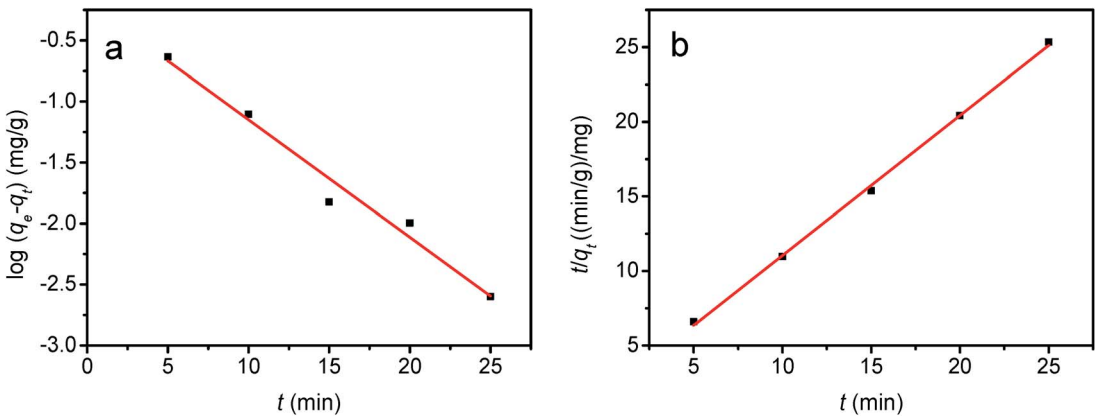

Fig. 6 Pseudo-first-order (a) and pseudo-second-order (b) models for the adsorption of cadmium onto $Cu_3(BTC)_2$–SO_3H.

3.5. Desorption of cadmium and recyclability of $Cu_3(BTC)_2$–SO_3H

$Cu_3(BTC)_2$–SO_3H can be readily regenerated and recycled, and it can retain more than 85% of the initial cadmium adsorption capacity after six cycles (Fig. 7). The preservation of its structural integrity after six adsorption/elution cycles has been confirmed by powder X-ray diffraction studies as shown in Fig. 8. N_2 isotherms of $Cu_3(BTC)_2$–SO_3H and $Cu_3(BTC)_2$–SO_3H after each recycle are shown in Fig. S3 (ESI†). Although the porosity of the $Cu_3(BTC)_2$–SO_3H was gradually lost in the subsequent adsorption/desorption cycle, the introduction of –SO_3H functional groups onto the pore surface of $Cu_3(BTC)_2$ can extend the application of water-unstable MOFs in terms of high adsorption capacity and selectivity for cadmium removal. Moreover, the regeneration could be easily achieved by washing the adsorbent with 50 mL deionized water, and then dried at 100 °C in an oven for 0.5 h before use.

3.6. Effect of background ions

Given their coexistence in wastewater, the effect of other metal ions (*i.e.*, Na^+, Mg^{2+}, Ca^{2+}, Pb^{2+}, Cu^{2+}, and Ni^{2+}) on cadmium removal efficiency of $Cu_3(BTC)_2$–SO_3H was assessed. As shown in Fig. 9, $Cu_3(BTC)_2$–SO_3H can retain its cadmium removal efficiency when various concentrations of metal ions solutions was added in 1 mg L^{-1} cadmium solution. It is noteworthy that the cadmium removal efficiency only decreased to 95.1% even in the presence of 100 mg L^{-1} background metal ion solutions. The good selective removal of cadmium is mainly due to the functionalization of SO_3H. In the case of $Cu_3(BTC)_2$–SH, Pb(II) demonstrated a more significant suppressive effect on cadmium adsorption. The removal efficiency of cadmium obviously decreased to 80% when the Pb(II) concentration was more than 10 mg L^{-1}. When $Cu_3(BTC)_2$–SH was converted by oxidation into $Cu_3(BTC)_2$–SO_3H, the removal efficiency of cadmium gradually decreased to 95.1% with the higher Pb(II) concentrations up to 100 mg L^{-1}. These studies suggest that $Cu_3(BTC)_2$–SO_3H preferably binds Cd(II) ions over other metal ions, highlighting its potential in selectively removing cadmium from practical wastewater.

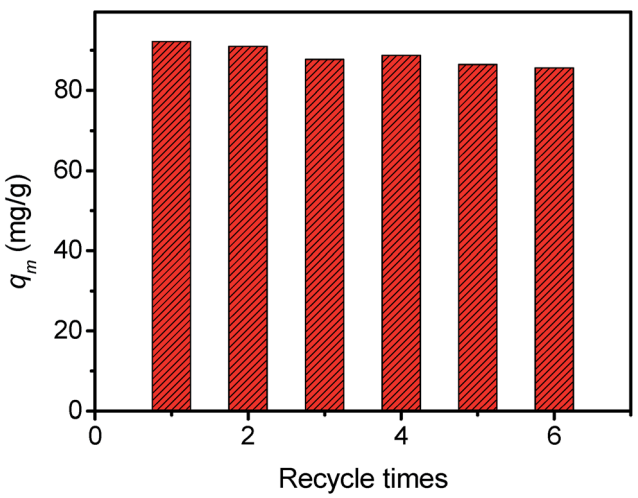

Fig. 7 Reusability of the $Cu_3(BTC)_2$–SO_3H for cadmium adsorption.

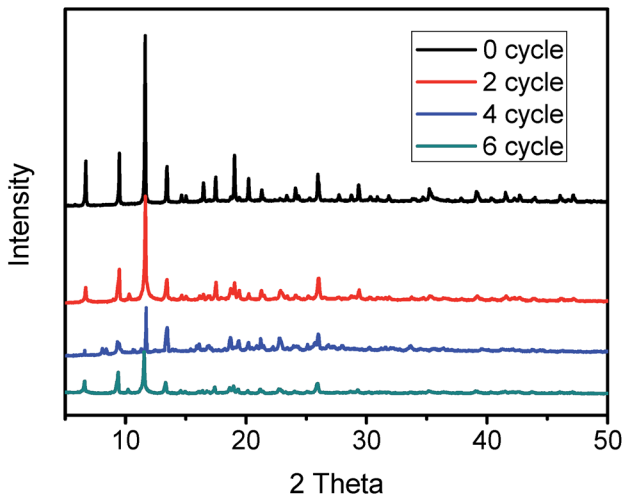

Fig. 8 Powder X-ray diffraction patterns for $Cu_3(BTC)_2$–SO_3H after 0, 2, 4, 6 adsorption/elution cycles.

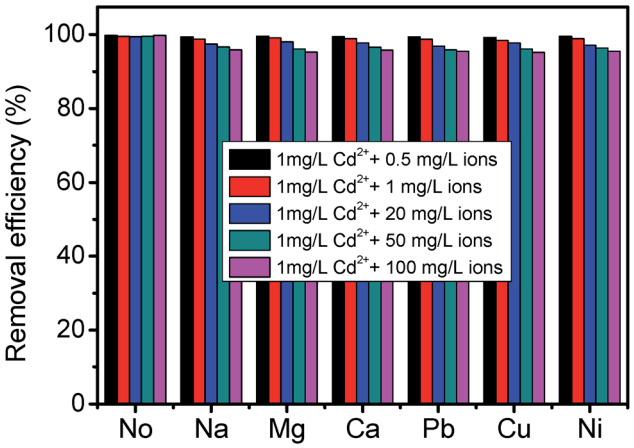

Fig. 9 Effect of coexisting ions on the removal of cadmium by $Cu_3(BTC)$–SO_3H.

4. Conclusions

We have demonstrated the anchoring of –SO_3H functional groups onto the pore surface of MOF for cadmium removal from aqueous solution as exemplified in the context of functionalizing the MOF, $Cu_3(BTC)_2$ with sulfonic acid *via* sequential post-synthetic modification and oxidation. The resultant sulfonic acid functionalized MOF, $Cu_3(BTC)_2$–SO_3H demonstrates high cadmium uptake capacity and fast kinetics for adsorbing cadmium ions from aqueous solution, outperforming the performances of some benchmark adsorbents. In addition, it exhibits high selectivity of cadmium ions in the presents of other background metal ions, and can be readily regenerated and recycled without significant loss of cadmium

uptake capacity. Our work therefore lays a foundation for developing functionalized MOFs as a new type of platform for removing cadmium from wastewater. Ongoing work in our laboratories includes the design of new MOFs for removing cadmium and other heavy metal ions for water treatment application.

Acknowledgements

This work was supported by the National Natural Science Foundation of China (21205103, 21275124), Jiangsu Provincial Nature Foundation of China (BK2012258), the Key Laboratory Foundation of Environmental Material and Engineering of Jiangsu Province (K13077) and a Project Funded by the Priority Academic Program Development of Jiangsu Higher Education Institutions. Partial support from the University of South Florida is also acknowledged (SM).

References

1 Z. Feng, S. Zhu, D. R. Martins de Godoi, A. C. S. Samia and D. Scherson, *Anal. Chem.*, 2012, **84**, 3764–3770.
2 M. P. Waalkes, *J. Inorg. Biochem.*, 2000, **79**, 241–244.
3 M. Xu, P. Hadi, G. Chen and G. J. McKay, *J. Hazard. Mater.*, 2014, **273**, 118–123.
4 I. A. Darwish and D. A. Blake, *Anal. Chem.*, 2001, **73**, 1889–1895.
5 J. Shao, J. D. Gu, L. Peng, S. Luo, H. Luo, Z. Yan and G. Wu, *J. Hazard. Mater.*, 2014, **272**, 83–88.
6 M. Kumar, B. P. Tripathi and V. K. Shahi, *J. Hazard. Mater.*, 2014, **273**, 118–123.
7 Y. Y. Ge, D. Xiao, Z. L. Li and X. M. Cui, *J. Mater. Chem. A*, 2015, **3**, 7666.
8 Y. B. Zhou, R. Z. Zhang and X. C. Gu, *J. Sep. Sci.*, 2015, **50**, 245–252.
9 H. T. Fan, J. X. Liu, H. Yao, Z. G. Zhang, F. Yan and W. X. Li, *Ind. Eng. Chem. Res.*, 2014, **53**, 369–378.
10 M. Machida, B. Fotoohi, Y. Amamo, T. Ohba, H. Kanoh and L. Mercier, *J. Hazard. Mater.*, 2009, **166**, 1067–1075.
11 C. Luo, R. Wei, D. Guo, S. Zhang and S. Yan, *Chem. Eng. J.*, 2013, **225**, 406–415.
12 C. J. Plaza, M. Viera, E. Donati and E. Guibal, *J. Environ. Manage.*, 2013, **129**, 423–434.
13 F. Ge, M. M. Li, H. Ye and B. X. Zhao, *J. Hazard. Mater.*, 2012, **211–212**, 366–372.
14 P. A. Amoyaw, M. Williams and X. R. Bu, *J. Hazard. Mater.*, 2009, **170**, 22–26.
15 S. Ma and H.-C. Zhou, *Chem. Commun.*, 2010, **46**, 44–53.
16 B. Li, K. Leng, Y. Zhang, J. Dynes, J. Wang, Y. Hu, D. Ma, Z. Shi, L. Zhu, D. Zhang, Y. Sun, M. Chrzanowski and S. Ma, *J. Am. Chem. Soc.*, 2015, **137**, 4243–4248.
17 K. Schlichte, T. Kratzke and S. Kaskel, *Microporous Mesoporous Mater.*, 2004, **73**, 81–88.
18 Y. C. Lin, Q. J. Zhang, C. C. Zhao, H. L. Li, C. L. Kong, C. Shen and L. Chen, *Chem. Commun.*, 2015, **51**, 697–699.
19 C. C. Zhao, C. Shen and W. Q. Han, *RSC Adv.*, 2015, **5**, 20386–20389.
20 F. Ke, L. G. Qiu, Y. P. Yuan, F. M. Peng, X. Jiang, A. J. Xie, Y. H. Shen and J. F. Zhu, *J. Hazard. Mater.*, 2011, **196**, 36–43.
21 Y. Wang, J. Xie, Y. Wu, H. Ge and X. Hu, *J. Mater. Chem. A*, 2013, **1**, 8782–8789.
22 G. S. Yang, Z. L. Lang, H. Y. Zang, Y. Q. Lan, W. W. He, X. L. Zhao, L. K. Yan, X. L. Wang and Z. M. Su, *Chem. Commun.*, 2013, **49**, 1088–1090.
23 B. Y. Li, Y. M. Zhang, D. X. Ma, Z. Shi and S. Ma, *Nat. Commun.*, 2014, **5**, 5537.
24 S. S. Chui, S. M. Lo, J. P. Charmant, A. G. Orpen and I. D. A. Williams, *Science*, 1999, **283**, 1148–1150.
25 A. U. Czaja, N. Trukhan and U. Muller, *Chem. Soc. Rev.*, 2009, **38**, 1284–1293.
26 D. Zuo, J. Lane, D. Culy, M. Schultz, A. Pullar and M. Waxman, *Appl. Catal., B*, 2013, **129**, 342–350.
27 E. P. Ng, S. N. M. Subari, O. Marie, R. R. Mukti and J. C. Juan, *Appl. Catal., A*, 2013, **450**, 34–41.
28 H. Zhang, W. P. Low and H. K. Lee, *J. Chromatogr. A*, 2012, **1233**, 16–21.
29 P. Chowdhury, C. Bikkina, D. Meister, F. Dreisbach and S. Gumma, *Microporous Mesoporous Mater.*, 2009, **117**, 406–413.
30 F. A. B. Silva and F. L. Pissetti, *J. Colloid Interface Sci.*, 2014, **416**, 95–100.
31 F. An, B. Gao, X. Dai, M. Wang and X. Wang, *J. Hazard. Mater.*, 2011, **192**, 956–962.
32 M. Xu, Y. Zhang, Z. Zhang, Y. Shen, M. Zhao and G. Pan, *Chem. Eng. J.*, 2011, **168**, 737–745.
33 A. Dubey, A. Mishra and S. Singhal, *Int. J. Environ. Sci. Technol.*, 2013, **11**, 1043–1050.
34 L. Bai, H. P. Hu, W. Fu, J. Wan, X. Cheng, Z. G. Lei, L. Xiong and Q. Chen, *J. Hazard. Mater.*, 2011, **195**, 261–275.
35 I. Langmuir, *J. Am. Chem. Soc.*, 1918, **40**, 1361–1403.
36 H. Freundlich, *Z. Phys. Chem.*, 1907, **57**, 385–470.
37 A. D. Kulynych and G. K. H. Shimizu, *CrystEngComm*, 2002, **4**, 102–105.
38 J. F. Song, Y. Chen, Z. G. Li, R. S. Zhou, X. Y. Xu, J. Q. Xu and T. G. Wang, *Polyhedron*, 2007, **26**, 4397–4410.
39 C. Y. Chen, C. L. Chiang and P. C. Huang, *Sep. Purif. Technol.*, 2006, **50**, 15–21.
40 O. Yalcinkaya, O. M. Kalfa and A. R. Turker, *J. Hazard. Mater.*, 2011, **195**, 332–339.
41 S. K. Lagergren, *Sven. Vetenskapsakad. Handl.*, 1898, **24**, 1–39.
42 S. Y. Ho and G. Mckay, *Process Biochem.*, 1999, **34**, 451–465.
43 N. Mirghaffari, E. Moeini and O. Farhadian, *J. Appl. Phycol.*, 2015, **27**, 311–320.
44 X. Y. Guo, B. Du, Q. Wei, J. Yang, L. H. Hu, L. G. Yan and W. Y. Xu, *J. Hazard. Mater.*, 2014, **278**, 211–220.
45 J. M. Duan and B. Su, *Chem. Eng. J.*, 2014, **246**, 160–167.
46 M. Zhang and H. Wang, *Int. J. Environ. Sci. Technol.*, 2014, **11**, 987–996.
47 X. L. Weng, S. Lin, Y. H. Zhong and Z. L. Chen, *Chem. Eng. J.*, 2013, **229**, 27–34.

